

Tableau 2. Principales distances interatomiques (Å) et angles de liaisons (°) dans  $\text{Na}_3\text{Sb}_3\text{As}_2\text{O}_{14}$ 

|  |           |   |           |
|--|-----------|---|-----------|
| Octaèdre Sb(1)O <sub>6</sub>                         |           | Octaèdre Sb(2)O <sub>6</sub>                  |           |
| Sb(1)—O(1)   | 1,94 (1)  | Sb(2)—O(7)                                    | 1,94 (1)  |
| —O(2)  | 1,97 (1)  | —O(7 <sup>III</sup> )                         | 1,96 (1)  |
| —O(5 <sup>I</sup> )                                  | 2,07 (1)  | —O(1)   | 1,98 (1)  |
| O(1)—Sb(1)—O(1 <sup>II</sup> )                       | 180,0     | —O(2)   | 1,99 (1)  |
| —O(2 <sup>III</sup> )                                | 94,1 (3)  | —O(4)   | 2,02 (1)  |
| —O(5 <sup>III</sup> )                                | 90,8 (3)  | —O(3)   | 2,04 (1)  |
| O(2)—Sb(1)—O(2 <sup>III</sup> )                      | 180,0     | O(7)—Sb(2)—O(7 <sup>III</sup> )               | 171,4 (1) |
| —O(5 <sup>I</sup> )                                  | 92,1 (3)  | —O(1)   | 94,7 (3)  |
| O(5)—Sb(1)—O(5 <sup>III</sup> )                      | 180,0     | —O(2)   | 84,0 (3)  |
|  |           | —O(4)   | 97,4 (3)  |
|  |           | —O(3)   | 87,6 (3)  |
| Tétraèdre AsO <sub>4</sub>                           |           | O(7 <sup>III</sup> )—Sb(2)—O(1)               | 83,9 (3)  |
| As—O(6 <sup>III</sup> )                              | 1,65 (1)  | —O(2)   | 98,0 (3)  |
| —O(3)  | 1,71 (1)  | —O(4)   | 91,0 (3)  |
| —O(4)  | 1,72 (1)  | —O(3)   | 83,9 (3)  |
| —O(5)  | 1,73 (1)  | O(1)—Sb(2)—O(2)                               | 176,5 (3) |
| O(6 <sup>III</sup> )—As—O(3)                         | 114,0 (4) | —O(4)   | 87,2 (3)  |
| —O(4)  | 116,5 (4) | —O(3)   | 90,1 (3)  |
| —O(5)  | 110,6 (4) | O(2)—Sb(2)—O(4)                               | 89,7 (3)  |
| O(3)—As—O(4)   | 99,2 (4)  | —O(3)   | 93,1 (3)  |
| —O(5)  | 108,9 (4) | O(4)—Sb(2)—O(3)                               | 174,5 (3) |
| O(4)—As—O(5)   | 106,9 (4) |   |           |
| Polyèdres Na(1)O <sub>6</sub> et Na(2)O <sub>8</sub> |           | O(1 <sup>I</sup> )—Na(2)—O(1 <sup>III</sup> ) | 180,0     |
| Na(1)—O(6 <sup>I</sup> )                             | 2,32 (1)  | —O(6 <sup>I</sup> )                           | 106,5 (3) |
| —O(3)  | 2,32 (1)  | —O(7)   | 119,2 (2) |
| —O(6 <sup>III</sup> )                                | 2,40 (1)  | —O(2)   | 61,3 (2)  |
| —O(5 <sup>I</sup> )                                  | 2,59 (1)  | O(6 <sup>I</sup> )—Na(2)—O(6 <sup>III</sup> ) | 180,0     |
| —O(2)  | 2,69 (1)  | —O(7)   | 85,7 (2)  |
| —O(4)  | 2,80 (1)  | —O(2)   | 92,7 (2)  |
| Na(2)—O(1 <sup>I</sup> )                             | 2,53 (1)  | O(7)—Sb(2)—O(7 <sup>II</sup> )                | 180,0     |
| —O(6 <sup>I</sup> )                                  | 2,54 (1)  | —O(2 <sup>II</sup> )                          | 121,2 (2) |
| —O(7)  | 2,67 (1)  | O(2 <sup>I</sup> )—Sb(2)—O(2 <sup>II</sup> )  | 180,0     |
| —O(2)  | 2,69 (1)  |   |           |

Code de symétrie: (i)  $\frac{1}{2}+x, \frac{1}{2}-y, z$ ; (ii)  $-x, -y, -z$ ; (iii)  $\frac{1}{2}-x, \frac{1}{2}+y, -z$ .

**Polyèdres Na(1)O<sub>6</sub> et Na(2)O<sub>8</sub>.** Le cation Na<sup>+</sup>(1) est situé dans un environnement octaédrique déformé d'oxygènes. Le cation Na<sup>+</sup>(2) exerce une coordinence bipyramidale à base hexagonale assez régulière (Tableau 2). Ces polyèdres partageant des sommets et des arêtes, forment une chaîne dans le canal parallèle à c.

La comparaison de cette structure avec celle du composé de formulation analogue  $\text{K}_3\text{Sb}_3\text{P}_2\text{O}_{14}$  (Piffard, Lachgar & Tournoux, 1985) montre que dans

cette dernière se manifestent les mêmes couches d'octaèdres  $\text{SbO}_6$  mais elles ne sont pas reliées entre elles par les tétraèdres  $\text{PO}_4$ : ces derniers ne mettant des sommets en commun qu'avec des octaèdres de la même couche. Nous attribuons cette modification structurale au rayon de l'ion  $\text{K}^+$  qui provoque un écartement des feuillets ne permettant pas à l'élément P ou As de former des liaisons avec deux couches successives.

Pour confirmer cette hypothèse, nous avons procédé à la synthèse de  $\text{Na}_3\text{Sb}_3\text{P}_2\text{O}_{14}$  et de  $\text{K}_3\text{Sb}_3\text{As}_2\text{O}_{14}$  qui se sont révélés effectivement être isotopes respectivement de  $\text{Na}_3\text{Sb}_3\text{As}_2\text{O}_{14}$  et de  $\text{K}_3\text{Sb}_3\text{P}_2\text{O}_{14}$  avec les caractéristiques radiocristallographiques suivantes:  $\text{Na}_3\text{Sb}_3\text{P}_2\text{O}_{14}$ : monoclinique;  $a = 12,579$  (9);  $b = 7,224$  (4);  $c = 6,216$  (3) Å;  $\beta = 107,60$  (5)°;  $\text{K}_3\text{Sb}_3\text{As}_2\text{O}_{14}$ : rhomboédrique;  $a = 7,219$  (2);  $c = 3,155$  (2) Å.

Au cours de la rédaction du présent mémoire, nous avons appris qu'une étude plus détaillée de la structure de  $\text{K}_3\text{Sb}_3\text{M}_2\text{O}_{14}$  (M: P, As) a été effectuée par Piffard et col. (à paraître dans *J. Solid State Chem.*). Elle confirme cette isotopie.

Le composé du titre a révélé des propriétés d'échange d'ions en solution acide. Une étude systématique est en cours.

#### Références

- BUSING, W. R., MARTIN, K. O. & LEVY, H. A. (1979a). *ORXFLS4. Crystallographic Structure-Factor Least-Squares Program*. Oak Ridge National Laboratory, Tennessee, EU.
- BUSING, W. R., MARTIN, K. O. & LEVY, H. A. (1979b). *ORFFE4. Crystallographic Function and Error Program*. Oak Ridge National Laboratory, Tennessee, EU.
- DRISS, A. (1979). Thèse de spécialité. Univ. de Tunis.
- DUNG, HUY-NGUYEN & JOUINI, T. (1978). *Acta Cryst.* B34, 3727–3729.
- HADDAD, A., GHEDIRA, M. & JOUINI, T. (1986). *C. R. Acad. Sci.* 303, 661–663.
- International Tables for X-ray Crystallography* (1974). Tome IV. Birmingham: Kynoch Press. (Distributeur actuel Kluwer Academic Publishers, Dordrecht.)
- MAGNÉLI, A. (1953). *Acta Chem. Scand.* 7, 315–324.
- PIFFARD, Y., LACHGAR, A. & TOURNOUX, M. (1985). *J. Solid State Chem.* 58, 253–256.

*Acta Cryst.* (1988). C44, 1157–1162

## Melt Growth and Characterization of Lead-Doped Crystals of Cadmium Iodide

BY U. P. TYAGI AND G. C. TRIGUNAYAT

Department of Physics and Astrophysics, University of Delhi, Delhi-7, India

(Received 6 November 1987; accepted 8 March 1988)

**Abstract.** A systematic study of the effect of doping metallic lead and lead iodide into cadmium iodide has been carried out. Both material purification and the

growth of doped single crystals have been carried out by the method of zone melting. The crystals have been characterized by X-ray diffraction and physical

methods. The doping affects the hardness and cleavage of the crystals. All Pb-doped crystals consist of the most common polytype 4H, but some of the  $\text{PbI}_2$ -doped crystals have also shown the presence of three higher polytypes. The X-ray photographs of the Pb-doped crystals show no 'streaking' and 'arcing', but nearly half of the  $\text{PbI}_2$ -doped crystals show 'streaking'. Also the exposure time for  $\text{PbI}_2$ -doped crystals was found to increase by an order of magnitude.

**Introduction.** The growth of polytypes of a compound depends on several factors such as temperature, pressure, rate of crystallization, nature of solvent, external field, presence of impurities, etc. Of these, the effects of temperature and rate of crystallization have been explored extensively, whereas the effects of other factors have been studied to a lesser extent. Regarding the effect of impurities, several different workers have reported the influence of impurities on the growth of SiC polytypes (Lundqvist, 1948; Hayashi, 1960; Knippenberg & Verspui, 1969; Mitomo, Inomata & Tanaka, 1971; Vodakov, Mokhov, Roenkov & Anikin, 1979). According to them the presence of various kinds and amounts of impurities results in the stabilization of different polytype structures. In another richly polytypic compound, ZnS, it has been reported that addition of various impurities induces structural transformations (Kozielski, 1975; Sebastian & Krishna, 1983; Krishna & Sebastian, 1986). Of late, Chaudhary & Trigunayat (1982*a,b*, 1987) have carried out a qualitative study of the effect of purification on the polytypism of  $\text{CdI}_2$ , which has emerged as the most richly polytypic compound in the last three decades. The well purified melt-grown  $\text{CdI}_2$  crystals did not show any polytypism at all.

It was planned to carry out a quantitative study of the effect of incorporation of impurities on the growth of  $\text{CdI}_2$  polytypes, by employing impurities of a known nature as well as of a known amount. As a first logical step, the raw  $\text{CdI}_2$  compound had to be well purified and then a given impurity had to be doped into it. To make the study as exact as possible, the dopants had to be chosen discriminately by carefully examining their relevant physical properties in relation to the properties and crystal structure of  $\text{CdI}_2$ . Further, only such dopants had to be chosen whose atoms/ions could play a significant role in bonding with the atoms/ions of Cd and I in the structure. The best interaction could possibly be achieved by replacement of the atoms/ions of the host material with the atoms/ions of the dopant, i.e. by the formation of a substitutional solid solution. To give the maximum possibility for such a formation, the following properties of dopants were scanned in relation to cadmium iodide: electropositivity, ionic radius, crystal structure of the resulting compound of the dopant and valency. Accordingly, metallic lead and lead iodide were chosen as the dopants.

**Experimental.** The method of zone levelling was employed to carry out the doping. It was preferred to the method of Bridgman–Stockbarger because when densities of the dopant and the host material differ substantially and solubility of the dopant in the host material is small the doping remains highly localized in the latter case. However, it is necessary that the melting point of the dopant is nearly the same as that of the host material. This condition was satisfied in the present case (the respective m.p.'s of Pb,  $\text{PbI}_2$  and  $\text{CdI}_2$  are 600, 675 and 661 K). Before doping, the host material, viz cadmium iodide, was well purified using the zone-refining technique. The technique has already been successfully employed earlier by Chaudhary & Trigunayat (1982*b*). The apparatus essentially consists of an outer cylindrical quartz jacket, a quartz boat for holding the charge, and resistance heaters mounted on a trolley moveable along guide rails. The experiments were performed in an atmosphere of argon gas, flowing in the direction of movement of the zone. Two circular heaters were employed for the creation of molten zones, so that one pass of the trolley effectively amounted to two zone passes over the material. About 1 cm length of the zone (the smallest manageable length) was allowed to pass through the charge at a speed of  $2 \text{ cm h}^{-1}$ . Twenty zone passes were used to purify the material. Only the extremely pure initial part of the ingot was used for the purpose of doping.

The same apparatus was adapted for zone levelling, after incorporating some modifications. Both forward and reverse movement of the zones were provided for. To ensure single-crystal formation in the final zone pass, irrespective of the direction of motion of the zones, both ends of the boat were tapered.

3 at. % of spectroscopically pure metallic lead was placed at one end of the boat containing purified  $\text{CdI}_2$ . A molten zone was created at this end and allowed to pass through the ingot at a speed of  $1.2 \text{ cm h}^{-1}$ . The molten lead sat at the bottom of the zone in the form of a globule and moved through the ingot along with the zone. Repeated-pass zone levelling, comprising four forward and backward passes, was adopted to achieve uniform doping, at the end of which the colour of the ingot was uniformly dull lemon yellow. The lead globule did not disappear but only reduced in size. The yellow colour of the ingot indicated local formation of  $\text{PbI}_2$ , which was confirmed by chemical analysis.

After the zone-levelling operation, single crystals of lead-doped cadmium iodide were grown in the same boat, by giving the final pass with a low-temperature gradient in the solid at the growth interface. Fig. 1 shows the temperature profile of the growth chamber during the final pass.

For promoting greater doping of lead, it was decided to employ  $\text{PbI}_2$  as the dopant, since  $\text{Pb}^{2+}$  ions ought to have higher reactivity than Pb atoms. Extremely pure  $\text{PbI}_2$ , well purified by zone refining, was used. In this

case, the speed of zone movement had to be reduced to  $8 \text{ mm h}^{-1}$ , to obtain a sharp solid-liquid interface and to avoid constitutional supercooling. 3 at. %  $\text{PbI}_2$  was used and 12 forward and backward passes were performed. A single crystal was grown as before, with the same temperature profile as shown in Fig. 1. It was yellow, except at the starting end, where it appeared translucent.

The doped single crystals were characterized by physical and X-ray diffraction methods. Their characteristics were compared with those of the melt-grown well purified undoped crystals of cadmium iodide, which are soft, transparent, colourless and amenable to easy basal cleavage. The intermediate major portion of the doped ingot, which had a clear transparent appearance, was chosen for the study.

Both Pb-doped and  $\text{PbI}_2$ -doped crystals were found to be harder, but the latter were found to be exceptionally hard.

As already mentioned, the uniformity of doping was broadly judged by examining the colour of different parts of the ingot. It was further tested by measuring the d.c. conductivity of several crystal pieces from different parts of the central portion of the ingot. The conductivity values were found to be almost the same, thus confirming a uniform distribution of the dopant in the ingot.

Unlike the undoped crystals, cleavage of the crystals doped with  $\text{PbI}_2$  was found to be much more difficult, whereas the cleavage in the crystals doped with metallic lead remained as easy as in the undoped cadmium iodide.

The optical perfection of the crystals was ensured before their X-ray examination. Small pieces, having thickness nearly  $\frac{1}{2}$ –1 mm and measuring nearly  $4 \times 5$  mm across, were cleaved along the basal plane from different parts of the ingot. Both basal faces of a given

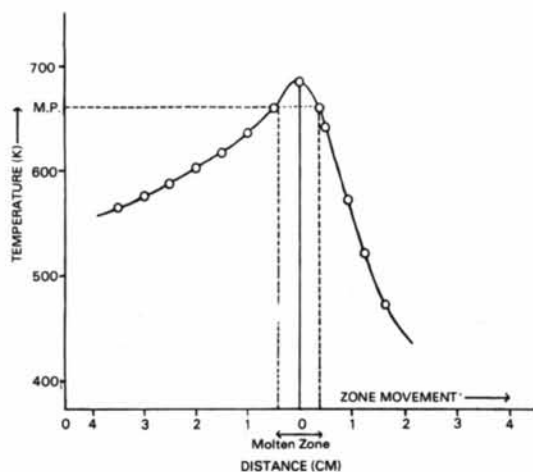


Fig. 1. Temperature profile of the growth chamber for growing Pb-doped  $\text{CdI}_2$  crystals by zone melting.

crystal were found to be shining. As for the undoped  $\text{CdI}_2$  crystals, the shining cleavage plane of a doped crystal was found to be perpendicular to the  $c$  axis. Further, the direction of the  $c$  axis was found to be perpendicular to the direction of the growth of the crystal.  $15^\circ$ -oscillation photographs of the crystals about the  $a$  axis were taken. Since the crystals of cadmium iodide are known to exhibit syntactic coalescence of polytypes, X-ray photographs of the two basal faces were separately taken. Since the  $\text{CdI}_2$  crystals also exhibit parallel growth of two or more polytypes on the same face, the photographs were taken from different parts of the same face.

In the case of Pb-doped crystals, eight crystal pieces were examined, yielding 32 X-ray diffraction photographs. All the photographs exclusively showed reflections of the most common polytype  $4H$  (Fig. 2). Unlike the oscillation photographs of the crystals grown from solution, they were found to be practically free of 'streaking' between the consecutive reflections. The X-ray photographs also did not show any 'arcings'.

Similarly, eight  $\text{PbI}_2$ -doped crystals were examined, yielding 48 X-ray photographs. Although none of the photographs showed 'arcings', 'streaking' was observed in 46% of cases. Eight photographs showed the presence of higher polytypes along with the basic type  $4H$ : one of the photographs showed the mixture ( $4H+12H+24H$ ) (Fig. 3), another showed the mixture ( $4H+8H+24H$ ) (Fig. 4) and the other six showed the presence of ( $4H+12H$ ) (Fig. 5). These crystals required much larger exposure times ( $\sim 10$ – $12$  h), compared with the undoped crystals ( $\sim 1$  h). Even the reflections recorded with 12 h exposure time appeared faint.

**Discussion.** As before, the results for the doped crystals are discussed in relation to the undoped crystals.

#### (i) Doping with metallic lead

That some lead was left behind in the form of a globule, after the operation of doping was completed, shows a limited solubility of lead in cadmium iodide. However, the structure of  $\text{PbI}_2$ , which is the compound locally formed as a result of substitution of Cd atoms by Pb atoms, is nearly identical with the structure of the



Fig. 2.  $a$ -axis  $15^\circ$ -oscillation photograph of a melt-grown Pb-doped crystal, showing reflections of the most common polytype  $4H$ . 3 cm camera;  $\text{Cu K}\alpha$  radiation.

host material,  $\text{CdI}_2$ . Further, the valency of lead, in the present case, also matches the valency of cadmium. Consequently, the only factor responsible for the observed limited solubility seems to be the difference between the ionic radii of the two metal ions ( $\text{Cd}^{2+}$ : 0.97;  $\text{Pb}^{2+}$ : 1.20 Å).

The observed increased hardness of the crystals can be accounted for as follows. Doping with lead results in the substitution of some of the Cd atoms by Pb atoms.

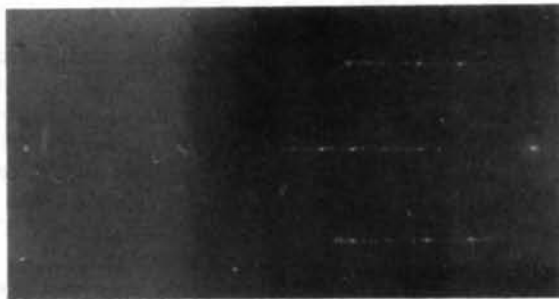


Fig. 3. *a*-axis 15°-oscillation photograph of a melt-grown  $\text{PbI}_2$ -doped crystal, showing reflections of the polytypes 4H + weak 12H + very weak 24H. Other conditions same as for Fig. 2.

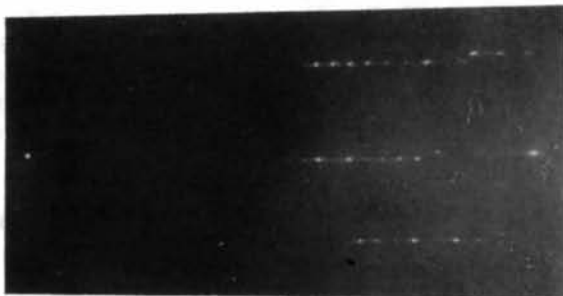


Fig. 4. *a*-axis 15°-oscillation photograph of a melt-grown  $\text{PbI}_2$ -doped crystal, showing reflections of the polytypes 4H + weak 8H + very weak 24H. Other conditions same as for Fig. 2. (The setting of the crystal is not perfect, but it poses no problem in the identification of polytypes.)



Fig. 5. *a*-axis 15°-oscillation photograph of a melt-grown  $\text{PbI}_2$ -doped crystal, showing reflections of the polytypes 4H + 12H. Other conditions same as for Fig. 2.

It is well known that a real crystal always contains mosaic blocks. Also, in the  $\text{CdI}_2$  structure half of the total number of octahedral voids, formed as a result of close packing of  $\text{I}^-$  ions, are empty. The replaced Cd atoms can enter into either the boundary between the mosaic blocks or the empty octahedral voids between the I–Cd–I sandwiches. Their first choice should be the mosaic boundaries, since that will change neither the dimensions of the unit cell nor the crystal structure substantially, thus producing little change in the free energy of the crystal. They will usually enter the interstitial octahedral voids when accommodation ceases to be available in the mosaic boundaries. When that happens, the bonding between the molecular sandwiches, which are normally held together by weak van der Waals forces, will become stronger (because now an intervening Cd atom will be weakly attracted by the  $\text{I}^-$  ions on both the sides), resulting in the observed hardening of the crystal. The occupancy of the interstitial sites will also affect the ease with which one layer may slip over another, which in turn will affect the hardness, malleability and ductility of the material (Lee, 1977). The strengths of Cd–I and Pb–I bonds are  $138 \pm 20$  and  $196 \pm 38$   $\text{kJ mol}^{-1}$ , respectively, at 298 K (Gaydon, 1968). Thus the  $\text{I}^-$  ions are expected to make a stronger bond with the substituting  $\text{Pb}^{2+}$  ions as compared to the  $\text{Cd}^{2+}$  ions, which will also contribute towards the hardening of the crystal. It may be added that in the molten state both cadmium and iodine will exist in ionic form. Further, in the molten state lead can also acquire ionic form because of its low ionization potential and the prevailing high temperature. The electrons released in the ionization can combine with the  $\text{Cd}^{2+}$  ions to produce Cd atoms. Thus, in the present case of metallic lead doping, cadmium is located in the interstitial sites in atomic form.

All crystals were the most common polytype 4H and their X-ray photographs were found to be practically free of 'streaking' and 'arcing'. In the earlier work on phase transformations in  $\text{CdI}_2$  polytypes, it was established that all polytypes tend to transform into 4H upon heating at high temperatures (Lal & Trigunayat, 1970, 1971, 1974) and that undoped melt-grown  $\text{CdI}_2$  crystals solely consist of the type 4H. In the melt growth, the crystals necessarily form at high temperatures. The exclusive existence of polytype 4H in the Pb-doped crystals shows that the doping does not affect the high-temperature stability of 4H. The 'streaking' arises from the existence of random stacking faults in the structure. Its absence on the X-ray photographs reveals that no faults exist in the Pb-doped crystals. The 'arcing' arises from the arrangement of edge dislocations into tilt boundaries (Agrawal & Trigunayat, 1969). Its absence indicates that either the density of the dislocations is small in the Pb-doped crystals or the dislocations are not arranged into small-angle tilt boundaries.

(ii) *Doping with lead iodide*

Compared with the previous case of doping with metallic lead, the addition of lead iodide will also lead to a partial substitution of  $\text{Cd}^{2+}$  ions by  $\text{Pb}^{2+}$  ions in the molecular sandwiches  $\text{I}-\text{Cd}-\text{I}$ . But now cadmium will be released in the structure as  $\text{Cd}^{2+}$  ions, instead of the electrically neutral Cd atoms. Since lead is already present in ionic form in the molten cadmium iodide, the process of ionization is not involved in this case and therefore a greater number of  $\text{Cd}^{2+}$  ions are likely to be released. As before, these ions will enter into the mosaic boundaries and the vacant interstitial sites between the sandwiches. All available  $\text{Pb}^{2+}$  ions may not be utilized in substituting for  $\text{Cd}^{2+}$  ions. Consequently, in addition to the released  $\text{Cd}^{2+}$  ions, the surplus  $\text{Pb}^{2+}$  ions will also occupy the octahedral voids and the mosaic boundaries. Further, in this case the constituent  $\text{I}^-$  ions of the dopant material will also be rendered surplus after the  $\text{Pb}^{2+}$  ions have dispersed in the structure. These ions will also tend to move into the mosaic boundaries and the vacant octahedral voids. Both  $\text{Cd}^{2+}$  and  $\text{Pb}^{2+}$  ions existing in the octahedral voids between two neighbouring sandwiches will make strong local bonds with the neighbouring  $\text{I}^-$  ions of the sandwiches. Consequently, the  $\text{PbI}_2$ -doped crystals are expected to be harder than the Pb-doped crystals, as actually observed. Another factor will contribute to hardening, *viz* the large ionic radii of  $\text{Pb}^{2+}$  and  $\text{I}^-$ , which have the values 1.20 and 2.16 Å, respectively (*cf.* the ionic radius of  $\text{Cd}^{2+}$  ions = 0.97 Å). The existence of such large ions will naturally make it difficult to compress the crystal. The increased bonding between the sandwiches will also render the cleavage of the crystal difficult, which also agrees with observation.

*Prima facie*, it may appear difficult for large  $\text{I}^-$  ions to enter the octahedral voids between the sandwiches. However, as the crystal is actually growing (*i.e.* the process is not occurring in an already grown crystal) and the surplus  $\text{I}^-$  ions have to be accommodated somewhere, the  $\text{I}^-$  ions are likely to be trapped in the voids. The attraction of the neighbouring interlayer  $\text{Cd}^{2+}$  cations, although weak, will facilitate such trappings.

A significant experimental observation for the  $\text{PbI}_2$ -doped crystals is that they require an extremely large exposure time (~10–12 h) to produce X-ray photographs with diffraction spots of appreciable intensity compared with the usual exposure time of 1 h for the undoped crystals. The radius of the sphere representing an octahedral void, obtained as a result of closest packing of  $\text{I}^-$  ions, is  $\approx 0.9$  Å. It implies that an ion of radius about 1 Å can enter the octahedral voids without producing any appreciable local displacements. In the present case, the radius of a  $\text{Pb}^{2+}$  ion (1.2 Å), entering into an octahedral void either by substituting for a  $\text{Cd}^{2+}$  ion (0.97 Å) or otherwise, is appreciably greater than that of a  $\text{Cd}^{2+}$  ion, *viz* by a factor of nearly 25%.

Consequently, strong local disturbances will be produced in the host structure. In addition, any  $\text{I}^-$  ions, which have a much larger radius (2.16 Å), entering into the vacant octahedral voids will produce even larger local disturbances. It is known that local displacements in a crystal structure lead to weakening of intensity of X-ray reflections (Vainshtein, Fridkin & Indenbom, 1982). Thus the local displacements caused by the introduction of the  $\text{Pb}^{2+}$  and  $\text{I}^-$  ions will result in the weakening of the intensity of X-ray reflections and hence in prolonging the exposure time, as actually observed.

Unlike the undoped and Pb-doped crystals, the X-ray study of the  $\text{PbI}_2$ -doped crystals has occasionally revealed the presence of higher polytypes. 'Streaking' has also been observed on 46% of the photographs. As mentioned earlier, the introduction of relatively large-sized  $\text{Pb}^{2+}$  and  $\text{I}^-$  ions in the  $\text{CdI}_2$  structure produces marked local distortions in the structure. Consequently, strong local internal stresses are built up in the structure. A natural way for the structure to relieve itself of such stresses is by creation of one or more edge dislocations at the stress positions. The crystal structure of  $\text{CdI}_2$  particularly favours the creation of edge dislocations. This is so because molecular layers of  $\text{I}-\text{Cd}-\text{I}$ , held together by weak van der Waals forces of attraction, can easily slip under a small stress. The most likely slip plane in a crystal is always that in which the atoms are closest packed. Also, the slip tends to take place in the direction of closest packing. The most probable slip planes and slip directions in the  $\text{CdI}_2$  crystals are  $\{0001\}$  basal planes and  $\langle 11\bar{2}0 \rangle$  directions, respectively. The slip will create an edge dislocation lying in the basal plane and having a Burger's vector  $a/3 \langle 11\bar{2}0 \rangle$ . Such a dislocation can easily dissociate, on its own, into two half dislocations as

$$a/3 \langle 11\bar{2}0 \rangle = a/3 \langle 10\bar{1}0 \rangle + a/3 \langle 01\bar{1}0 \rangle,$$

*i.e.* a perfect dislocation transforms into two partial dislocations bounding a ribbon of stacking faults. The  $\text{CdI}_2$  structure favours slip in the  $\langle 10\bar{1}0 \rangle$  directions, too. Therefore, the partials may also be created independently. The movement of the partials also enlarges faulting along the basal plane, to the possible extent that the entire plane may become faulted. These processes result in the creation of randomly distributed stacking faults in the crystal, which manifest themselves as 'streaking' on the oscillation photographs. Because of thermodynamic factors or otherwise, sometimes the faults can arrange themselves in a regular fashion, leading to the formation of various polytypes (Trigunayat & Verma, 1976). This explains the observed occasional presence of higher polytypes in the crystals and the observed frequent existence of 'streaking' on the X-ray photographs.

## References

- AGRAWAL, V. K. & TRIGUNAYAT, G. C. (1969). *Acta Cryst.* A25, 401–407.
- CHAUDHARY, S. K. & TRIGUNAYAT, G. C. (1982a). *Cryst. Res. Technol.* 17, 465–468.
- CHAUDHARY, S. K. & TRIGUNAYAT, G. C. (1982b). *J. Cryst. Growth*, 57, 558–562.
- CHAUDHARY, S. K. & TRIGUNAYAT, G. C. (1987). *Acta Cryst.* B43, 225–230.
- GAYDON, A. G. (1968). *Dissociation Energies and Spectra of Diatomic Molecules*. London: Chapman and Hall.
- HAYASHI, A. (1960). *J. Mineral. Soc. Jpn*, 4, 363–371.
- KNIPPENBERG, W. F. & VERSPUL, G. (1969). *Mater. Res. Bull.* 4, S33–44.
- KOZIELSKI, H. J. (1975). *J. Cryst. Growth*, 30, 86–92.
- KRISHNA, P. & SEBASTIAN, M. T. (1986). *Bull. Mineral.* 109, 99–116.
- LAL, G. & TRIGUNAYAT, G. C. (1970). *Acta Cryst.* A26, 430–431.
- LAL, G. & TRIGUNAYAT, G. C. (1971). *J. Cryst. Growth*, 11, 177–181.
- LAL, G. & TRIGUNAYAT, G. C. (1974). *J. Solid State Chem.* 9, 132–138.
- LEE, J. D. (1977). *Concise Inorganic Chemistry*. London: Van Nostrand.
- LUNDQVIST, D. (1948). *Acta Chem. Scand.* 2, 177–191.
- MITOMO, M., INOMATA, Y. & TANAKA, H. (1971). *Mater. Res. Bull.* 6, 759–764.
- SEBASTIAN, M. T. & KRISHNA, P. (1983). *Solid State Commun.* 48, 879–882.
- TRIGUNAYAT, G. C. & VERMA, A. R. (1976). *Physics and Chemistry of Materials with Layered Structures*, Vol. 2, edited by F. LEVY, Dordrecht: Reidel.
- VAINSHTEIN, B. K., FRIDKIN, V. M. & INDENBOM, L. V. (1982). *Modern Crystallography II: Structure of Crystals*. New York: Springer-Verlag.
- VODAKOV, YU. A., MOKHOV, E. N., ROENKOV, A. D. & ANIKIN, M. M. (1979). *Pis'ma Zh. Tekh. Fiz.* 5, 367–370.

*Acta Cryst.* (1988). C44, 1162–1164

### Diaquabis[tetrachloroaurate(III)-Cl<sup>1</sup>, Cl<sup>2</sup>]zinc(II)

BY PETER G. JONES, RALF SCHELBACH, EINHARD SCHWARZMANN AND CARSTEN THÖNE

*Institut für Anorganische Chemie der Universität, Tammannstrasse 4, 3400 Göttingen,  
Federal Republic of Germany*

(Received 25 January 1988; accepted 8 March 1988)

**Abstract.** [Zn(AuCl<sub>4</sub>)<sub>2</sub>(H<sub>2</sub>O)<sub>2</sub>],  $M_r = 779.0$ , monoclinic,  $P2_1/n$ ,  $a = 7.576$  (2),  $b = 12.113$  (2),  $c = 15.355$  (3) Å,  $\beta = 103.51$  (2)°,  $V = 1370.1$  Å<sup>3</sup>,  $Z = 4$ ,  $D_x = 3.78$  Mg m<sup>-3</sup>,  $\lambda(\text{Mo } K\alpha) = 0.71069$  Å,  $\mu = 24.7$  mm<sup>-1</sup>,  $F(000) = 1376$ ,  $T = 293$  K. The structure was refined to  $R = 0.034$  for 2057 unique observed reflections. Discrete [Zn(AuCl<sub>4</sub>)<sub>2</sub>(H<sub>2</sub>O)<sub>2</sub>] molecules are observed; the coordination geometry at Zn is distorted octahedral and at gold square-planar. The water ligands are mutually *cis*. Two Cl atoms of each AuCl<sub>4</sub> ion bridge to zinc; the bridging Au–Cl bonds are appreciably longer than their non-bridging counterparts.

**Introduction.** Our recent studies of tetrachloroaurate(III) salts have involved both monatomic (Tl, Na) and polyatomic (SbCl<sub>3</sub>, SeCl<sub>3</sub>, TeCl<sub>3</sub>, PCl<sub>4</sub>) cations (Jones, Schelbach & Schwarzmänn, 1987a; Jones, Hohbein & Schwarzmänn, 1988; Jones, Jentsch & Schwarzmänn, 1988; Jones, Schelbach & Schwarzmänn, 1987b; Jones, Jentsch & Schwarzmänn, 1986; Freire Erdbrügger, Jones, Schelbach, Schwarzmänn & Sheldrick, 1987). Many other crystallographic studies of AuCl<sub>4</sub><sup>-</sup> salts have been performed; for a summary, see Jones (1981, 1983, 1986).

Two tetrachloroaurates of zinc have been described in the literature. von Bonsdorff (1829) reported a

dodecahydrate that was 'stable even in fairly moist air'. Topsøe (1874) reported an octahydrate that deliquesced even in quite dry air. It is not clear if these compounds are in fact identical.

We wished to ascertain if anhydrous zinc bis(tetrachloroaurate) exists. 100 mg gold(III) chloride and 45 mg zinc chloride (Fluka purum p.A., anhydrous) were sealed in a glass ampoule under nitrogen in 4 ml AsCl<sub>3</sub> as solvent. The ampoule was heated to 373 K for 12 h and allowed to cool. Two types of crystal separated; red (Au<sub>2</sub>Cl<sub>6</sub>) and yellow (the title compound). The nature of the yellow product was established by this structure determination. Because the compound is very moisture sensitive, crystals were sealed in glass capillaries under inert oil.

**Experimental.** A crystal 0.15 × 0.12 × 0.04 mm was used to record 4595 profile-fitted intensities (Clegg, 1981) on a Stoe–Siemens four-circle diffractometer (monochromated Mo K $\alpha$  radiation,  $2\theta_{\text{max}} 50^\circ$ , hemisphere  $\pm h \pm k \pm l$ ). Three check reflections showed no significant intensity change. An absorption correction based on  $\psi$  scans was applied; transmissions ranged from 0.31 to 0.67. Merging equivalents gave 2400 unique reflections ( $R_{\text{int}} 0.025$ , index range  $h -9$  to  $+8$ ,  $k 0$  to  $14$ ,  $l 0$  to  $18$ ), 2057 of which with  $F > 4\sigma(F)$  were